ChemComm

FEATURE ARTICLE

View Article Online
View Journal | View Issue

Cite this: *Chem. Commun.*, 2025, **61**, 232

Development and application of ordered membrane electrode assemblies for water electrolysis

Nian Hua, Chuanyan Zhang, Wenjie Zhang, Xinyun Yao and Huidong Qian *

With the development of hydrogen energy, there has been increasing attention toward fuel cells and water electrolysis. Among them, the zero-gap membrane electrode assembly (MEA) serves as an important triple-phase reaction site that determines the performance and efficiency of the reaction system. The development of efficient and durable MEAs plays a crucial role in the development of hydrogen energy. Consequently, a great deal of effort has been devoted to developing ordered MEAs that can effectively increase catalyst utilization, maximize triple-phase boundaries, enhance mass transfer and improve stability. The research progress of ordered MEAs in recent advances is highlighted, involving hydrogen fuel cells and low temperature water electrolysis technology. Firstly, the fundamental scientific understanding and structural characteristics of MEAs based on one-dimensional nanostructures such as nanowires, nanotubes and nanofibers are summarized. Then, the classification, preparation and development of ordered MEAs based on three-dimensional structures are summarized. Finally, this review presents current challenges and proposes future research on ordered MEAs and offers potential solutions to overcome these obstacles.

Received 8th October 2024,
Accepted 25th November 2024

DOI: 10.1039/d4cc05300a

rsc.li/chemcomm

1. Introduction

In the past decades, due to the increasing use of fossil fuels and greenhouse gas emissions, environmental problems have been arising on the earth.[1–5] Thus, there is an urgent need to develop and use sustainable clean energy to solve the environmental pollution problem caused by the excessive use of fossil fuels. Hydrogen has potential as an energy carrier due to its high-energy, environmental friendliness, storability and sustainability.[6–13] However, until now, most hydrogen has been produced through reforming of natural gas or other fossil fuels under certain conditions, which is called gray or blue hydrogen and is accompanied by the production of carbon dioxide byproducts.[14–17] Therefore, exploring efficient green hydrogen production technology is a crucial route to reduce carbon emissions and thus achieve carbon neutrality.[18] Splitting of water into green hydrogen and oxygen using electricity transforms water into a sustainable and

Department of Chemistry, College of Sciences, Shanghai University, Shanghai 200444, China. E-mail: qianhd@shu.edu.cn

Nian Hua

Nian Hua was born in Guangxi, China in 2001. He received his Bachelor of Engineering degree from Central South University (China) in 2024. Currently, he is studying for his master's degree under the supervision of Prof. Huidong Qian at the College of Sciences, Shanghai University (China). His research focuses on the preparation and applications of bipolar membranes and membrane electrode assemblies.

Chuanyan Zhang

Chuanyan Zhang was born in Shandong, China in 2002. She received a Bachelor of Science degree from Ningxia University in China in 2024. At present, she is studying for a master's degree at the School of Science of Shanghai University under the supervision of Prof. Huidong Qian. Her primary research area is fuel cells.

environmentally friendly fuel source, which has attracted the attention of many researchers and companies.[19,20] At present, there are some problems such as high production costs and immature production technology. These problems hinder the development of hydrogen production *via* water electrolysis and hydrogen energy utilization.[21–23]

In order to reduce the production cost of green hydrogen and improve the yield and purity of hydrogen, scientists are committed to the research of low-temperature water electrolysis (WE) technology.[24–27] At present, the widely used technologies are alkaline water electrolysis (AWE), proton exchange membrane water electrolysis (PEMWE), and anion exchange membrane water electrolysis (AEMWE) (Fig. 1).[28] MEA is a component with a zero-gap sandwich structure in low temperature hydrolysis technology which is composed of a polymer membrane in the middle and a catalytic layer (CL) and liquid/gas diffusion layer (L/GDL) on both sides. This special structure can effectively reduce mass transfer resistance and interface resistance, improve the efficiency of WE, and ensure stable operation.[29,30] However, the preparation of MEAs requires materials that can endure high applied voltage

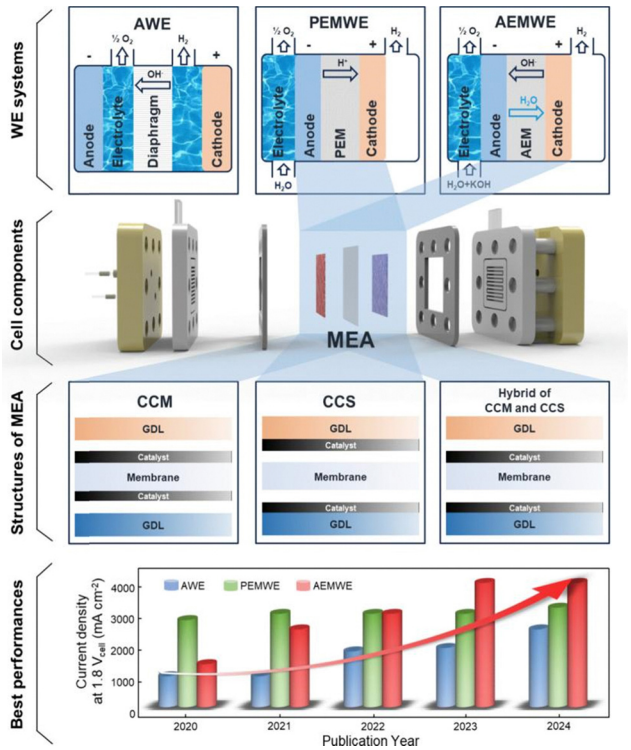

Fig. 1 Schematic images of WE systems, a cell configuration, the three types of MEA structures (CCS, CCM, and CCS/CCM hybrid), and the current densities at 1.8 V for each WE system over the past five years. Reproduced with permission from ref. 28. Copyright 2024 American Chemical Society.

(~2.0 V) and high current density. This is bound to bring high production costs, which can hinder the industrialization and development of water electrolysis technology.[31,32] In terms of MEA preparation methods, both the catalyst coated substrate (CCS) and the catalyst coated membrane (CCM) will face significant challenges in terms of high manufacturing costs and low catalyst utilization.[33,34]

Wenjie Zhang

Wenjie Zhang was born in Sichuan, China in 1999. She obtained her Bachelor of Science degree in Applied Chemistry from Nanjing Tech University (China) in 2024. Presently, she is pursuing her master's degree under the guidance of Prof. Huidong Qian at the College of Sciences, Shanghai University (China). Her research is centered on the application of bipolar membranes in flow batteries.

Xinyun Yao

Xinyun Yao graduated from Nanjing University of Information Science and Technology in 2015 with a Bachelor of Science degree. After that, she worked in the field of chemistry for 6 years. She is currently pursuing a Master's of Chemistry at the School of Science, Shanghai University with Professor Qian Huidong as a supervisor. Her main research direction is bipolar membrane water electrolysis.

Huidong Qian

Prof. Huidong Qian earned a PhD in 2014 at Key Laboratory of Polymer Ecomaterials, Changchun Institute of Applied Chemistry, Chinese Academy of Sciences (CAS). He then started his research work on ion exchange membranes at Shanghai Advanced Research Institute, CAS before moving to Shanghai University in 2023. His current research interest focuses on developing key components and device for water electrolysis, fuel cells and flow batteries, including proton exchange membranes, anion exchange membranes, bipolar membranes and membrane electrode assemblies.

In order to solve the problems of how to improve the efficiency of electrolysis and reduce the load of noble metals, scientists have conducted a lot of studies. Designing an ordered MEA with a maximum triple-phase boundary, a larger membrane/CL interface and a fast mass transfer channel is an effective way to solve the above problems. Compared with the traditional MEAs, the ordered MEAs have good performance due to the advantages of less catalyst loading, more catalyst active sites, and effective reduction of mass transfer resistance. The hydrophobic nature of conventional MEA CLs leads to gas coverage at the catalytic sites, hindering the triple-phase boundary and reducing efficiency. In contrast, ordered MEAs exhibit aerophobicity and super-hydrophilicity, facilitating gas desorption through a defined path and allowing for easier electrolyte penetration.[35] This unique property significantly enhances performance, particularly in high current density regions where gas evolution is more pronounced. It has been widely used in the field of fuel cells.[36,37] Since the year of 2001, there has been a steady increase in the number of yearly reports on ordered MEAs mainly for fuel cells (Fig. 2). The MEAs based on nanostructured Pt-based thin film (NSTF) catalysts developed by 3M Company are the most typical ordered nanostructured MEAs in the fuel cell field and the first implemented on a commercial scale.[38–41] Nowadays, the ordered MEAs are also gradually being applied to the field of hydrogen production by WE, and a variety of nanostructured MEAs is constantly developed and designed. This is also of great significance for promoting the development of WE technology, which provides more active surface area, thus increasing the contact area between the electrode and the electrolyte, increasing the energy density and greatly improving the hydrolysis efficiency. This optimized ordered design also leads to better catalyst utilization, reducing material waste and contributing to cost reduction. It lays a solid foundation for the future commercial application of WE technology. Despite the promising benefits of ordered MEAs, their widespread adoption is currently hindered by several challenges. The intricate fabrication process demands meticulous control over temperature, pressure, and solution concentration, leading to high equipment and material costs. This complexity also makes large-scale production difficult, limiting scalability for commercial applications. Furthermore, maintaining the stability and durability of ordered MEAs during long-term recycling remains a significant issue.

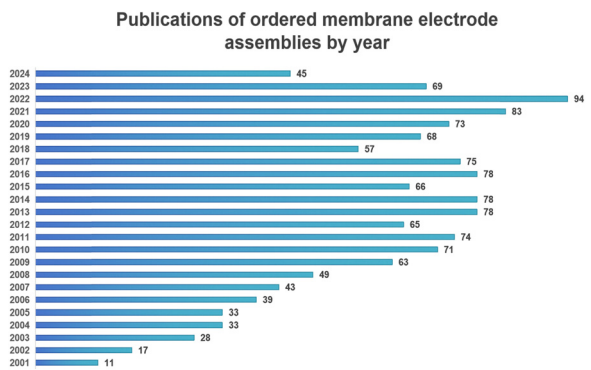

Fig. 2 Number of reports of ordered membrane electrode assemblies over the years from Clarivate. 2024 encompasses Jan–Sep.

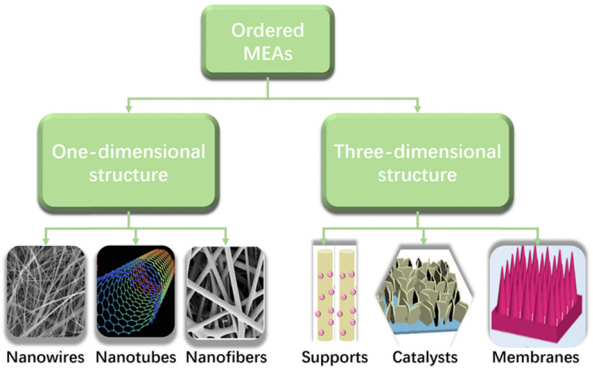

Fig. 3 General framework of the feature article.

In this feature article, we review the research and development of ordered MEAs, and summarize the advantages and disadvantages of various preparation methods. The types of ordered MEAs based on one-dimensional nanostructures in the early stage of development and their applications in fuel cells and WE for hydrogen production are briefly introduced. The classification of the 3D ordered MEAs and domestic and foreign research status in the field of hydrogen production by WE is highlighted. Finally, the future developments and challenges associated with new generation ordered MEAs are discussed. The framework of this feature article is displayed in Fig. 3.

2. Nanostructured MEAs based on 1D nanostructures

Although the conventional MEA performance is very effective for improving the performance of fuel cells and WE, the practical application of MEAs needs to solve the problems of low catalyst utilization, limited catalytic active site, blocked mass transfer and high ohmic resistance. In the early development stage of ordered MEAs, with the continuous development of nanowire materials, researchers tried to combine them with the preparation of MEAs, mainly including ordered support nanotube materials (mainly carbon nanotubes), catalyst nanowires (mainly Pt nanowires) and high proton conduction nanofibers (mainly Nafion wires) (Fig. 4).[42] The reason why nanowire materials are widely used in MEAs is that they can increase the specific surface area of the catalysts and improve the material transport capacity to a certain extent, so the comprehensive performance of the MEAs can be effectively improved. This section describes the development of nanostructured MEAs based on 1D nanostructures in the fields of fuel cells and WE.

2.1 MEAs based on nanowires

As an effective electrocatalyst, Pt-based nanowires are widely used in fuel cells.[43–45] In addition, nanostructured MEAs based on 1D nanowires have been shown to exhibit improved

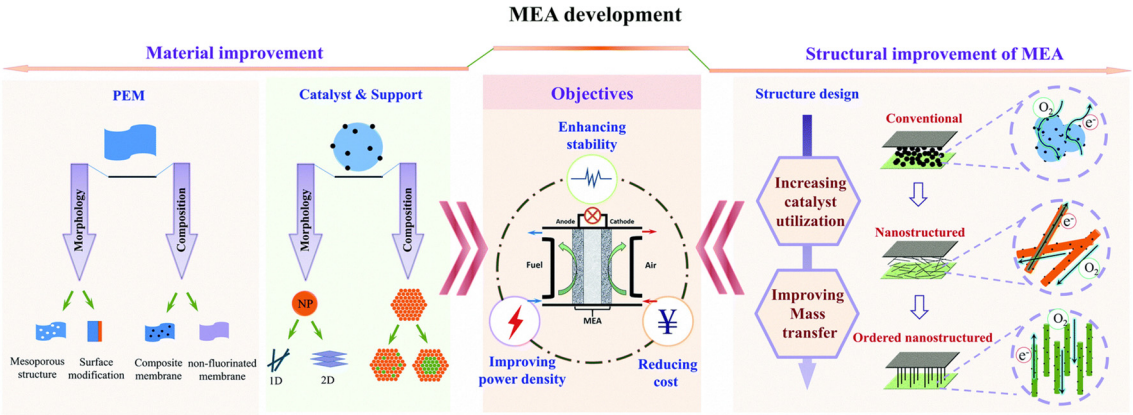

Fig. 4 The trend of the development of nanostructured MEAs. Reproduced with permission from ref. 42. Copyright 2019 Royal Society of Chemistry.

MEA performance.[46,47] Specifically, due to its special crystal surface and fewer surface defects, the catalyst nanowires have a higher specific oxygen reduction activity (1.5 times that of traditional Pt/C catalysts),[48] which can better adapt to the requirements of large-scale production. Sun *et al.* developed a simple wet chemical method for growing single crystal platinum nanowires on carbon black nanospheres in an aqueous solution at room temperature.[49] The density of Pt nanowires on the carbon support was controlled by adjusting the mass ratio of Pt precursor to carbon support. Furthermore, the length of the Pt nanowires could be adjusted by controlling the growth time. The resulting Pt NW/C catalyst demonstrated a 50% increase in mass activity and a threefold improvement in specific activity compared to conventional Pt nanoparticle (NP) catalysts. However, other studies have observed that due to the lower specific surface area of 1D Pt NWs compared to some commercial carbon-supported Pt NPs, MEAs with 1D Pt NWs exhibit a smaller electrochemically active surface area (ECSA) than a conventional MEA at low Pt loading.[50,51] Yu *et al.* compared the prepared Pt NWs with the commercialized 40 wt% Pt/C catalyst (JM) and Pt black using electrochemical testing methods.[52] It was found that although the catalyst nanowire showed lower ECSA than the commercial NPs, the ECSA reduction in the potential cycle aging test was much smaller than that of the ordinary Pt/C catalyst, and it had better stability.

In the research of hydrogen production by water electrolysis, Liang *et al.* constructed a stacked NiFe@NiFeOOH electrode using a magnetic field-assisted chemical deposition method (Fig. 5).[53] Ultrathin (~5 nm) and amorphous NiFeOOH were *in situ* formed on the surface of NiFe alloy nanowires. Studies have shown that oxygen bubbles easily leave the surface of nanowire arrays at small sizes. The unique micro- and nanoscale electrode design minimizes contact between the electrode and bubbles, improving the surface's hydrophilicity towards the electrolyte. This optimization leads to impressive performance, enabling current densities of 0.5 A cm^{-2} and 1.0 A cm^{-2} with low overpotentials of 248 mV and 258 mV, respectively. Transition metal alloys, particularly NiW, exhibit inherent catalytic activity and abundant surface area, making them highly effective for hydrogen evolution reactions (HERs) in alkaline conditions.[54] However, these alloys face durability and corrosion resistance challenges in acidic conditions. Kim *et al.* loaded NiW alloy onto Cu nanowires (NWs). This highly porous structure enhances corrosion resistance and catalytic activity in HER.[55] The Cu NWs, electrodeposited on carbon paper, provide a large surface area and numerous loading sites for the NiW catalyst. The resulting NiW/Cu NW electrode demonstrates exceptional catalytic activity, achieving a current density of 10 mA cm^{-2} at an overpotential of 56 mV.

2.2 MEAs based on nanotubes

Carbon nanotubes (CNTs) have gained widespread use as catalyst supports in fuel cell applications due to their exceptional properties, including high specific surface area, excellent electrical conductivity, and unique pore structure.[56–59] Compared with traditional carbon materials, CNTs offer advantages in electrode performance, exhibiting a higher electrocatalyst utilization rate, enhanced electron conduction, optimized mass transfer pathways, and superior resistance to high-potential corrosion.[60] These attributes make CNTs the optimal choice for carbon support materials. Hsieh *et al.* successfully synthesized Pt/CNTs using a pulsed microwave-assisted polyol method, resulting in uniformly distributed Pt NPs (2–3 nm) on the CNT surface.[61] This enhanced the mass specific power density of the Pt/CNT MEA to 5.45 kW g_{Pt}^{-1} in an H_2/O_2 PEMFC (80 °C), almost doubling the performance of commercial MEAs (1.9 kW g_{Pt}^{-1}). However, achieving stable Pt deposition on CNT surfaces remains a challenge. Fang and colleagues addressed this by employing a urea-assisted deposition method on sodium dodecyl sulfate (SDS)-modified multi-walled carbon nanotubes (MWCNTs).[62] The ECSA of Pt/SDS-MWCNTs was 83 m^2 g^{-1}, about 48% higher than that of conventional Pt/C (56 m^2 g^{-1}). The maximum power density of Pt/SDS-MWCNT based MEA was 451 mW cm^{-2}, much higher than those of conventional ones.

CNTs are also being widely studied and applied in the field of WE. Hu *et al.* reported a hollow array of $FeCo_2S_4$ nanotubes (Fig. 6).[63] Due to the unique hollow nanotube structure, the catalyst exposes more active sites and promotes charge transfer.

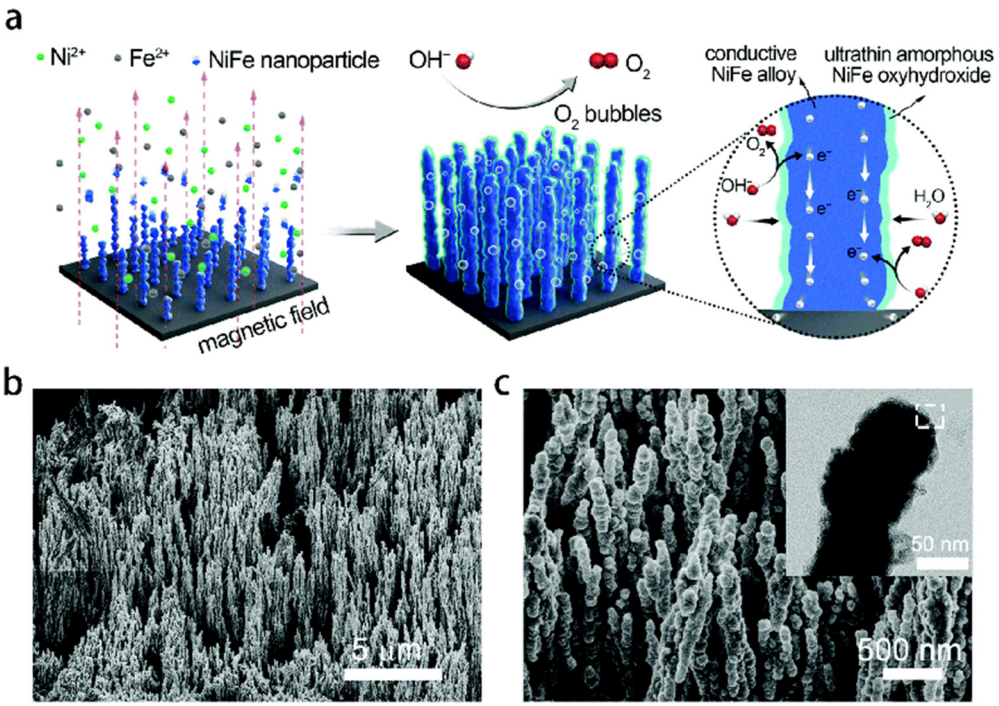

Fig. 5 (a) Schematic of the synthesis of the Ni_xFe_{1-x}–AHNA nanowire array and its function for OER. (b) and (c) SEM images of Ni_xFe_{1-x}–AHNAs at different magnifications. The inset of (c) is a low magnification TEM image of a single nanowire. Reproduced with permission from ref. 53. Copyright 2020 Royal Society of Chemistry.

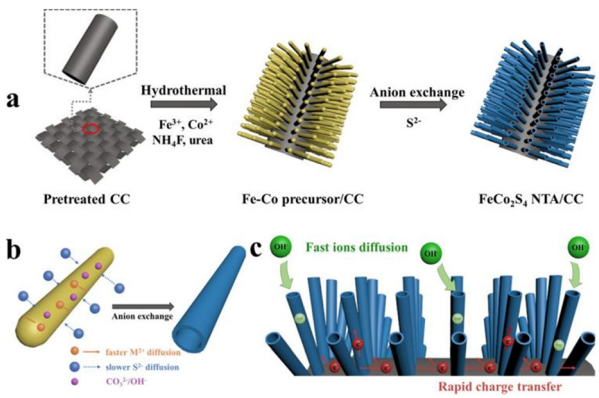

Fig. 6 (a) and (b) Schematic illustrations of the synthesis of the $FeCo_2S_4$ nanotube arrays supported on CC through a two-step method by anion exchange reactions. (c) Schematic diagram of the rapid electron/ion transportation within the $FeCo_2S_4$ NTA/CC electrode during OER process. Reproduced with permission from ref. 63. Copyright 2019 American Chemical Society.

The results show that the prepared electrode can provide a current density of 10 mA cm^{-2} under an overpotential of 278 mV, and has good electrochemical efficiency. Holzapfel *et al.* introduced a hybrid catalyst $[Mo_3S_{13}]^{2-}$ cluster (Mo_3S_{13}-NCNT) anchored to N-doped CNTs for HER under acidic conditions.[64] In a 0.5 M H_2SO_4 solution, the catalyst achieved a current density of 10 mA cm^{-2} at an overpotential of 188 mV and a Tafel slope of about 40 mV dec^{-1}, showing excellent catalytic performance.

2.3 MEAs based on nanofibers

Similar to carbon nanotubes, carbon nanofibers (CNFs) have unique electrical and structural properties that have great potential in the application of ordered MEAs.[65–67] Li *et al.* found that porous CNFs (PCNFs) have a variety of pore sizes and a relatively rough surface, which enables better loading of Pt catalysts.[68] They synthesized PCNF nanostructured electrodes by electrospinning and carbonization. The length of the prepared PCNFs is 0.5 to 2 mm, the average diameter is 150 nm, and Pt NPs can be evenly distributed on the surface. Compared with traditional Pt/C electrodes, Pt/PCNF exhibited better electrocatalytic activity and durability, and Pt/PCNF based MEA also exhibited improved battery performance compared with conventional ones, which provided direction for the development and utilization of CNFs in ordered MEAs. In order to improve the efficiency of proton channel transport in MEAs, high proton conduction nanodimensions were also introduced. Choi *et al.* prepared a nanofiber network membrane of proton exchange polymers by electrospinning technology, which has better proton transport performance than ordinary proton exchange membranes.[69,70] The nanofiber mat is prepared by electrospinning technology, compressed to form a membrane, and then the blank area of the membrane is filled with a polymer that does not affect the mass transfer. Pan *et al.* prepared Nafion–silica–HPW electrodes with different concentrations of Nafion.[71] The results show that when the content of Nafion is less than 30%, the electrode microstructure shows a sequence of 5–6 nm nanoarrays. When the temperature is 150–200 °C and

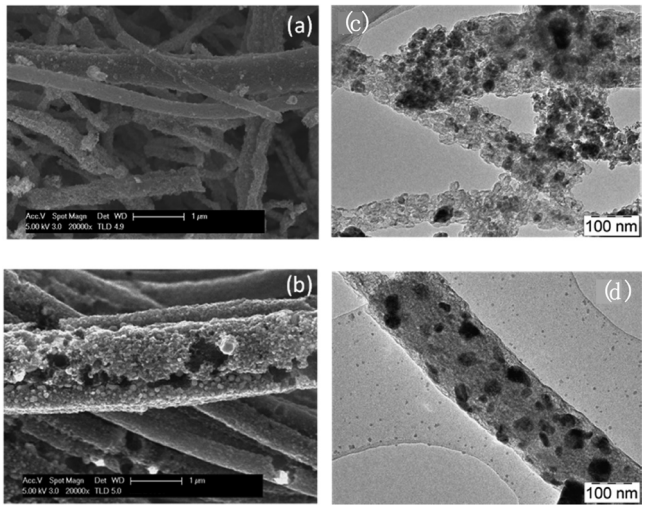

Fig. 7 SEM micrographs of the (a) $NiCo_2O_4$/CNF and (b) $NiMn_2O_4$/CNF anode catalysts. TEM micrographs of the (c) $NiCo_2O_4$/CNF and (d) $NiMn_2O_4$/CNF anode catalysts. Reproduced with permission from ref. 72. Copyright 2019 Elsevier.

the relative humidity (RH) is 25%, the proton conductivity can reach 0.082–0.095 S cm^{-1}, which is better than the traditional proton exchange membrane conduction efficiency.

Similarly, nanofiber technology has also been widely introduced into the study of ordered MEAs in WE. Busacca *et al.* prepared $NiMn_2O_4$ and $NiCo_2O_4$ electrocatalysts for oxygen evolution (OER) on carbon nanofibers by electrospinning (Fig. 7).[72] Experimental results show that the nanoscale electrocatalyst is uniformly dispersed on the nanocarbon fibers, which is conducive to the catalytic activity of the OER in alkaline hydroelectrolysis. The $NiMn_2O_4$ electrode showed high mass activity (362 A g^{-1}@1.8 V) in zero-gap AEMWE. Kang *et al.* also reported carbon-coated $Co_{0.9}Fe_{0.1}$ alloy NPs supported on carbon nanofibers (CNFs) for the OER.[73] The current density of the MEA with the $Co_{0.9}Fe_{0.1}$/CNF anode catalyst is 794 mA cm^{-2} at 1.7 V, which effectively improves the performance in alkaline WE.

These studies demonstrate the diverse and promising applications of 1D nanostructures in WE. Their unique structural and electronic properties contribute to the design of highly efficient catalysts, paving the way for the development of more sustainable and cost-effective hydrogen production methods.

3. Overall design of high performance ordered MEAs

The methods described above employ 1D nanostructures to organize the catalyst supports, electrocatalysts, and membranes of MEAs to varying degrees. While these approaches have led to improvements in MEA performance, significant challenges remain in achieving the overall ordered structure necessary for efficient, triple-phase mass transfer within MEAs. This section emphasizes another type of ordered MEAs that utilize 3D nanostructures, optimize triple-phase boundaries in the CLs, create triple-phase mass transfer pathways, and enhance the interfaces between membrane/CL and CL/GDL. Compared with 1D ordered MEAs, 3D ordered MEAs boast a more complex structure with the catalyst, electrolyte solution and GDL precisely arranged in 3D space. This design results in a more efficient triple-phase boundary and larger specific surface area, leading to superior energy conversion, material transport, catalyst utilization, and overall stability. However, the preparation process of 3D ordered MEAs is considerably more complex, demanding advanced technology and stringent control. In contrast, 1D ordered MEAs have a simpler structure and fabrication process, making them a more practical option. Therefore, 1D ordered MEAs and 3D ordered MEAs have different requirements under different conditions of use. The former is suitable for low requirements for preparation technology and transmission efficiency, while the latter is more suitable for high-performance and high-efficiency applications. The focus includes ordered catalyst supports and catalysts, and ordered membrane electrodes. Therefore, the overall design of the ordered MEAs is crucial for improving the electrochemical efficiency and reducing production costs.

3.1 Ordered design in supports

The introduction of ordering into catalyst supports of MEAs facilitates the directional arrangement of catalysts, improving the active site availability and catalyst utilization, while promoting the efficient transport of charges and substances.[74] For example, when CNTs are vertically oriented, electrons can move rapidly along the CNT direction with minimal energy loss. Electrochemical tests have showed ordered CNTs exhibit higher performance compared to unordered CNTs and conventional carbon supports at all current densities.[75] Hatanaka *et al.* developed a highly efficient fuel cell electrode by growing CNTs on a silicon substrate. They then deposited Pt NPs onto the CNT network by spraying and reducing Pt nitrate.[76] This catalyst was subsequently hot-pressed at 150 °C to form a robust MEA. The *I–V* curve and impedance spectrum data confirmed the remarkable material transport performance of the ordered CNT electrode, attributed to its enhanced diffusion pathways and efficient electron conductivity. Meanwhile, Chen *et al.* developed an ordered nanostructure MEA utilizing vertically aligned CNTs.[77] The ECSA of the prepared Pt/VACNT/Nafion/Pt/VACNT MEA was 78.72 m^2 g_{Pt}^{-1}, surpassing the value of 52.22 m^2 g_{Pt}^{-1} typical of conventional MEAs. The mass specific power density of the ordered nanostructured MEA reached 1.43 kW g_{Pt}^{-1}, representing a 50% increase compared to the conventional MEA (0.70 kW g_{Pt}^{-1}) in the PEMFC at 0.1 MPa and 80 °C. This innovative approach indicates the advantages of ordered structures in enhancing the overall efficiency of MEAs. Xuan *et al.* synthesized a TiN nanorod array on an ITO surface by a crystal seed assisted hydrothermal reaction followed by nitriding treatment, uniformly coating a Pt catalyst on the TiN support. This process successfully yielded a double-sided ordered MEA based on the TiN nanorod array.[78] The performance results indicated that with a Pt loading of 0.20 mg cm^{-2}, the double-sided ordered MEA achieved a peak power of 678.30 mW cm^{-2}. After 200 h of accelerated stress

testing (AST), the MEA's peak output decreased by only 4.8%, demonstrating that the double-sided ordered MEA effectively provides a specific mass transfer pathway, numerous catalyst loading sites and improved catalytic activity.

3M Company has developed an ordered array of nanostructured thin film (NSTF) electrodes with good performance for PEMWE. However, some studies on CL ordered arrays have only reported half-cell based performances.[79–81] Jiang *et al.* prepared an ordered array electrode as a feature of the defective Ir film decorated on external WO_x by electrodeposition nanorods (WO_xNRs) (Fig. 8).[82] An ordered array of WO_xNR was prepared on W foil by hydrothermal synthesis. Then, the Ir catalyst is coated on the outside of the WO_xNR ordered array using a combination of chronopotentiometry (CP) and cyclic voltammetry (CV). With the number of CV deposits ranging from 25 to 100, the loading capacity of the Ir coating on the ordered array can be 9–144 μg_{Ir} cm^{-2} and the thickness can reach 24–68 nm. Due to the high dispersibility of the Ir of the electrode, the Ir showed good catalytic activity. Vertically ordered CL provides efficient transport channels for substances. Due to the excellent stability of the WO_xNRs, the electrode material can run stably for 1030 h at 0.5 A cm^{-2}. Song *et al.* designed an integrated ultra-low PtIr CCM (IUCCM). Semi-ordered PtIr nanoflower arrays grown by wet chemistry were used as catalyst layers.[83] When IUCCM was successfully made into PEMWE, the test results showed that its current density at 1.77 V (2.0 A cm^{-2}) was greater than that of conventional CCM prepared by spray coating (1.2 A cm^{-2}). The Tafel slope value of IUCCM (39.8 mV dec^{-1}) is also significantly lower than that of the conventional CCM (67.5 mV dec^{-1}) described above, and the performance remains stable for 300 h at 0.5 A cm^{-2} and 80 °C. Therefore, IUCCM has faster dynamic properties, better water electrolysis performance and excellent stability. Zeng *et al.* constructed a novel cost-effective nanoporous ultrathin film (NPUF) OER electrode based on NPG/IrO_2 composites.[84] All the holes of the NPUF electrode have the characteristics of three-dimensional interconnection, and IrO_2 NPs are embedded in NPG to form composite ultra-thin films. They found that because the electrode has a 3D interconnected nanopore ratio, the gas can be easily separated, resulting in high mass transfer efficiency and electrocatalyst utilization. As the anode catalyst, the loading of IrO_2 and Au can reach 86.43 and 100.0 mg cm^{-2}, respectively. Its electrolytic voltage is 58 mV lower than that of conventional IR-loaded electrodes, and it remains relatively constant within 300 h (@250 mA cm^{-2}) with good durability. The new NPUF electrode has a good application prospect in PEMWE.

In contrast to powder catalysts, self-supported electrodes do not require the use of polymer binders, which prevents them from inhibiting the exposure of the catalyst's active site and the diffusion of gas liquids. The self-supported electrodes do not require external support, making them well-suited for WE catalytic reaction under high current densities and long-term operation. Additionally, self-supported electrodes display excellent corrosion resistance and durability. Common self-supporting electrode materials that can be directly grown on L/GDL include carbon cloth (CC), carbon paper (CP), metal mesh (such as Ni or stainless steel mesh), metal felt and metal foam (Ni foam).[85] For example, a FeOOH/NiFe LDH self-supporting electrode with a vertically aligned nanosheet structure was synthesized using hydrothermal methods (Fig. 9).[86] Ding *et al.* reported the preparation of Fe–Ni_3S_2 anodic electrocatalysts on Ni foam by one-pot hydrothermal reaction in alkaline conditions.[87] They found that as the hydrothermal temperature increased from 150 °C to 190 °C, the morphology of the Fe–Ni_3S_2 self-supported electrode transitioned from a rough irregular structure to a more ordered, layered nanowire structure. The Fe–Ni_3S_2/NF electrode has an overpotential of 302 mV at 1.0 A cm^{-2}.

Some advanced manufacturing techniques (*e.g.*, 3D printing) also can optimize MEA's architecture to improve gas diffusion and reduce mass transport limitations. Recently, 3D printing has enabled the manufacture of porous electrodes which cannot be machined using traditional methods. With micron-scale precision, the pore structure of an electrode can now be designed for optimal energy efficiency, and a 3D printed

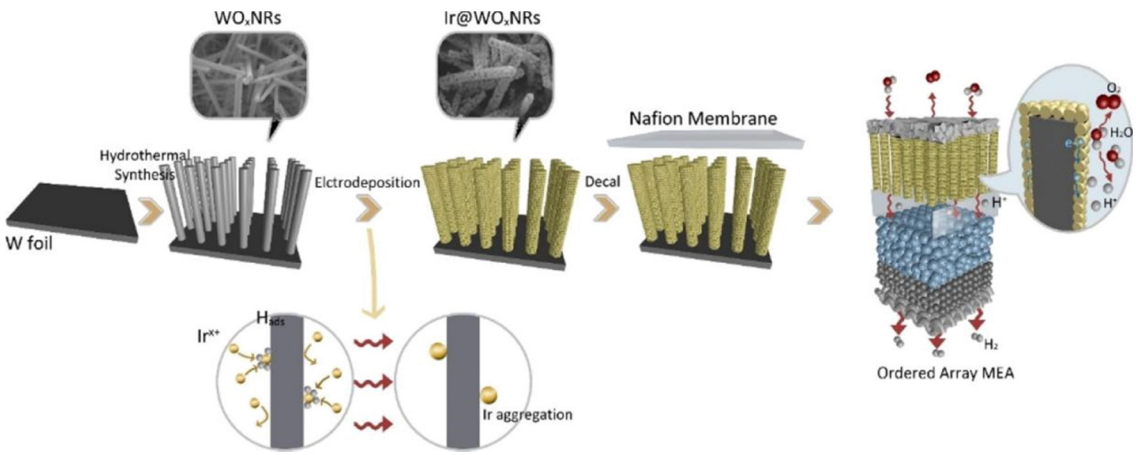

Fig. 8 Schematic diagram of the preparation and structure of the Ir@WO_xNR ordered electrode. Reproduced with permission from ref. 82. Copyright 2021 American Chemical Society.

Fig. 9 Schematic illustration of the formation process of the porous VA FeOOH/NiFe LDH-NF electrodes. Reproduced with permission from ref. 86. Copyright 2016 American Chemical Society.

electrode is not limited to a single uniform porosity. Davis *et al.* optimized the electrode structure to reduce the power loss in the flow reactor.[88] The computer-generated structure is then printed and benchmarked against a uniformly porous electrode. Biu *et al.* showed how the optimized electrode reduces the power requirement by 16% and look forward to the future application of this method to flow cells, electrolyzers and fuel cells to accelerate their development and implementation.[89] They used 3D printing to prepare porous flow electrodes in the electrolyzer, which is almost entirely manufactured by 3D printing. These electrodes were 3D printed using fused deposition modeling (FDM) of a composite material of conductive carbon and polylactic acid (PLA), and then electrodeposited on a Ni electrocatalyst. The stability and performance of the Ni-PLA electrode were tested in 1.0 M NaOH. Although the efficiency of these electrolyzers may not yet meet the thresholds required for commercial applications, they offer an innovative design strategy for new electrode preparation that has the potential to enhance performance and ensure the reliable operation of MEAs.

3.2 Ordered design in catalysts

Ordered catalysts, such as Pt nanotubes and Pt nanowires, are notable for their unique structural characteristics and improved performance compared to conventional power catalysts. Pt nanowires have specific crystal surfaces with fewer defects, leading to a specific activity that is 1.5 times greater than that of traditional Pt/C catalysts when employed as a CL. A significant advancement in the commercialization of ordered catalysts can be seen in 3M Company's approach. They utilize single-layer oriented organic dye whiskers as a catalyst support, onto which Pt is deposited *via* physical vapor deposition.[90–93] The unique structure of whisker-based catalysts offers several advantages over conventional Pt/C catalysts. Specifically, the whisker architecture helps to maintain the active catalyst area over time and withstand high potential conditions without degradation. Since these electrodes do not require carbon black or ionomers, they can be manufactured to be 20–30 times thinner than the ordinary Pt/C CLs. This ultra-thin design not only minimizes the amount of Pt used, effectively lowering manufacturing costs, but facilitates proton conduction under optimal conditions. In addition, the thin structure enhances the material transport capacity at high current densities, significantly improving the overall efficiency of hydrogen fuel cells.

Pan *et al.* employed a distinct approach, using electrodeposition to synthesize Pt nanowires with diameters of 60 nm and 25 nm within anodized aluminum oxide (AAO) templates.[94] CV tests showed that the Pt nanowire-array catalyst exhibited an electrochemically active surface area exceeding its geometric area. This highly ordered Pt nanowire-array catalyst facilitated both electron conduction and mass transport, resulting in a significant enhancement in oxygen reduction reaction (ORR) performance. Shao *et al.* developed an ordered MEA using a vertically aligned open-walled PtCo bimetallic NT array.[95] They grew vertically aligned Co–OH–CO nanowires on stainless steel plates by hydrothermal synthesis, and then coated Pt onto the Co–OH–CO nanowires by magnetron sputtering. Finally, the materials were annealed in a H_2/Ar atmosphere at temperatures of 300, 400 and 500 °C to obtain the open-walled PtCo bimetallic NT arrays. The catalytic activity of the as-prepared MEA was significantly improved in H_2/O_2 PEMFCs operating at 0.2 MPa and 80 °C, and its power density reached 14.38 kW g_{Pt}^{-1}, 1.7 times that of the traditional MEAs. In addition, the design of the open-walled structure contributes to exceptional durability by eliminating the need for carbon supports and ionomers, which often degrade over time.

Inspired by fuel cell technology, zero-gap MEA technology has been adopted for alkaline electrolyzers.[96] However, traditional MEA preparation methods typically involve spraying a catalytic ink containing catalyst powders, ionomers and solvents onto a porous L/GDL or membrane.[97] The CL structure obtained by this method suffers from several significant drawbacks: (1) limited mass transfer: the disordered and dense nature of the CL structure hinders the mass transport. (2) Reduced active sites: the addition of ionomers leads to a reduction in the catalyst active site, negatively impacting catalytic efficiency. (3) Electrolytic instability: the non-conductive, swellable and thermal instability of the polymer membranes can cause catalyst electrode detachment, affecting the electrolytic stability.[98,99] Recent research has concentrated on developing methods to create uniform and dense CLs on the membrane surface, aiming to enhance hydrogen production efficiency. However, directly constructing ordered CLs on the surface of ion exchange membranes remains a significant challenge.[100,101] Wang's group constructed an all-in-one MEA by using a solvothermal method to intergrow CoNi layered double hydroxide (LDH) nanosheet arrays on both sides of polypropylene porous membranes (Fig. 10).[102] They converted the CoNi LDH nanosheet arrays to CoNiS by a mild vulcanization treatment without changing the basic structure of the nanosheet arrays. The CL of the MEA has a large surface area, as well as an enhanced 3D ordered channel for gas–liquid mass transfer. There is no need to use polymer binders in the CLs, so the local oxygen transport is improved and the catalyst active site is more exposed. Due to the unique all-in-one design, the interface resistance between CL and the membrane is greatly reduced, and the conductivity is improved. The experimental results show a high current density of 1.0 A cm^{-2} achieved in

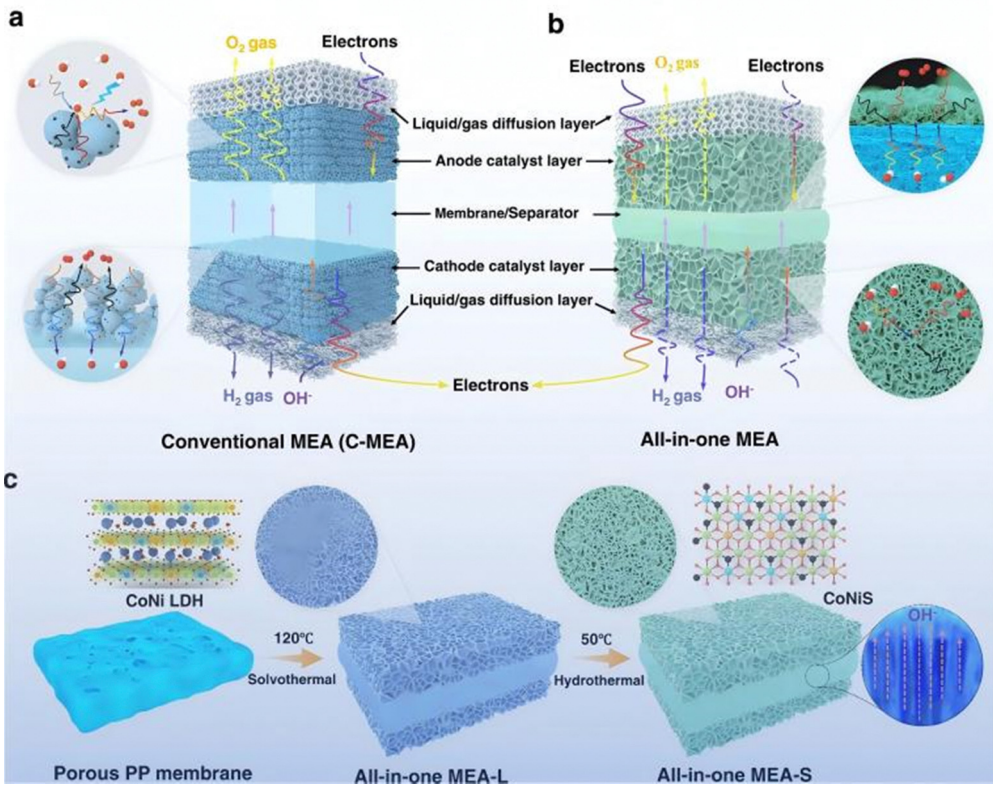

Fig. 10 Schematic illustration of the all-in-one MEA concept and preparation process. (a) Conventional MEA (C-MEA) and (b) all-in-one MEA based on 3D-ordered transport highways. (c) Synthetic procedure for the all-in-one MEAs. Reproduced with permission from ref. 102. Copyright 2022 Nature.

30 wt% KOH at 1.57 V with durability of more than 1000 h. This provides a new approach for developing high-performance alkaline WE. A novel 3D ordered MEA based on porous ordered CL, an ultra-thin ion exchange membrane and 3D CL/membrane interface structure has also been prepared by Wang's research group and applied to AEMWE.[103] The VCoP porous foams with highly ordered nanostructures were synthesized on aluminum foil (AF) by electrodeposition. This approach enabled the creation of a 3D interconnected interface between the CL and the membrane through direct film deposition technology, preserving the CL's ordered porous nanostructure throughout the process. This MEA design benefits from several key features: (1) a vertically ordered porous CL structure: facilitates efficient gas and liquid mass transfer. (2) An ultra-thin ion exchange membrane: minimizes ohmic resistance during mass transfer. (3) A 3D ordered CL/membrane interface structure: enhances the transport efficiency of hydroxide ions at the interface. These characteristics collectively contribute to the MEA's exceptional performance, achieving a high current density of 4.2 A cm^{-2} at 2.0 V in 1 M KOH. Recently, Wang's group proposed a swell-assisted transfer strategy to construct an ordered anode catalyst layer (Fig. 11).[104] By using a direct film deposition method to form a 3D interlocked CL/AWE interface, the ordered CL can be transferred to AEM at low temperature without damage, thus giving the MEA a vertically ordered CL structure. The strong bond formed between the interfaces contributes to the overall stability of the assembly,

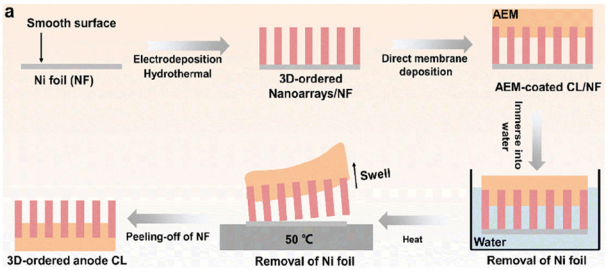

Fig. 11 Schematic diagram for the novel swell-assisted transfer method. Reproduced with permission from ref. 104. Copyright 2024 Royal Society of Chemistry.

making it feasible to remove the dense substrate. In a pure water environment, the AEMWE can reach a remarkable current density of 3.61 A cm^{-2} at 2.0 V. Furthermore, the system maintains stable operation for 700 h at 1.0 A cm^{-2}, indicating its reliability and efficiency for prolonged use.

3.3 Ordered design in membranes

Membrane ordering strategies can be divided into two categories: (1) regulating the internal microstructure of the membrane to form an orderly arrangement of proton transport channels, thereby improving the conductivity of MEAs. (2) Constructing ordered nanostructures on the surface of the membrane and expanding the triple-phase boundary to increase the catalyst active area and

improve the catalyst utilization rate. Nafion membrane is the most commonly used solid electrolyte for PEMFC and PEMWE because of its high proton conductivity and good chemical stability.[105,106] However, in actual production applications, its widespread application faces challenges, such as high production costs and sensitivity to harsh use environments, which hinder its large-scale development. In the past decades, various non-perfluorinated ion PEMs[107–111] and nanostructures PEMs[112–116] have been developed to try to solve the problems existing in Nafion membranes.

3.3.1 Constructing ionic highways in membranes. Elabd *et al.* prepared high-purity Nafion nanofibers by electrospinning.[117] After testing, the conductivity of the single root can reach 1.5 S cm^{-1} when the diameter is 400 nm, which is higher than the current commercial Nafion membrane (<0.1 S cm^{-1}). It was also found that the proton conductivity increased sharply with the decrease in nanofiber diameter, and at 30 °C, the RH changed from 50% to 90%, and the proton conductivity of Nafion nanofibers increased by two orders of magnitude. It is of great significance to improve the performance of PEM. Among the reported nanostructured PEMs, hydrophilic inorganic NPs (such as silica) have been extensively studied to modify Nafion membranes.[118,119] Wang *et al.* developed a composite film composed of a Nafion matrix and nanophosphonic acid functionalized silica by a sol–gel process.[120] Due to the synergistic interaction between acidic groups and porous silica, the nano-silica/Nafion membrane shows good proton conductivity and water retention, which may be the result of the synergistic interaction between acidic groups and porous silica. At 85 °C and 50% RH, the proton conductivity of the nano-silica/Nafion membrane is 0.026 S cm^{-1}, which is 24% higher than that of the ordinary Nafion membrane. Constructing mesoporous structures in the Nation matrix is another representative method for preparing nanostructured PEMs. The mesoporous Nafion membrane has good water retention, which simplifies water management and reduces operating costs.[121] Jiang *et al.* prepared a highly ordered mesoporous Nafion (mNafion) film by the micellar template method.[122] With PEO_{127}–PPO_{48}–PEO_{127} as a surfactant, it has excellent water retention, and the proton conductivity and water retention are significantly improved compared with traditional Nafion membranes.

In alkaline WE, there are two effective strategies to improve the conductivity of MEAs by increasing the ion exchange capacity (IEC) and constructing an ion high-speed channel in the membrane. However, an excessive increase in IEC can affect the mechanical properties and stability of the membrane, thus limiting the practical application of MEAs in alkaline WE. Although constructing ion fast channels in membranes is a daunting challenge, this is an ideal approach in comparison. Many literature reports have reported strategies for constructing high speed channel formation of ion conduction in AEMs.[123–129] Liu *et al.* proposed a strategy to mitigate membrane degradation by inducing polymer crystallization and regulating the local hydrophilic environment of organic cations (Fig. 12).[130] They replaced the alkyl side chain with the hydrophilic *N*-oligoethylene glycol (OEG) side chain and linked it

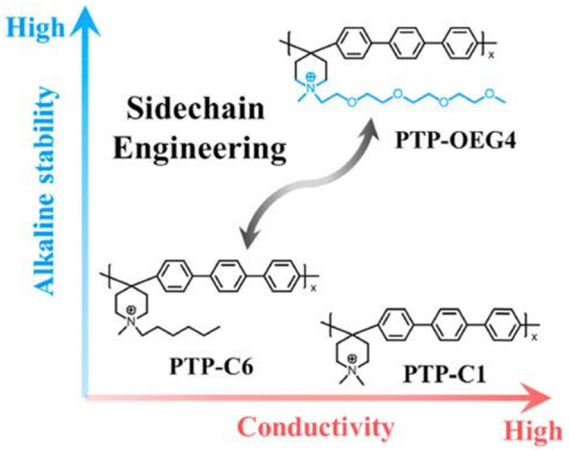

Fig. 12 The impact of side chain engineering on hydroxide conductivity and alkaline stability of AEMs. Reproduced with permission from ref. 130. Copyright 2023 Elsevier.

with the piperidine group (PTP-OEG) to prepare a comb-shaped poly(terphenyl piperidinium) (PTP) AEM for WE. The experimental and simulation results show that the stability, mechanical properties and electrical conductivity of the membrane are improved, which opens up a new way for the study of the ordered MEAs in AEMWE. Crosslinking strategies have proven effective in constructing high-speed ion channels within AEMs. Hu *et al.* demonstrated this by employing rigid crosslinkers to expand the interchain spacing of polymer chains.[131] Replacing these rigid crosslinkers with shorter, more flexible counterparts significantly enhanced hydroxide conductivity, increasing it from 63.2 to 110.3 mS cm^{-1} at 80 °C.

3.3.2 Constructing ordered structures on the membrane surface. Constructing a membrane surface ordered nanoarray is generally through *in situ* growth on the membrane. The ordered proton conductor array defines the three-phase material transport channel in CL and promotes the efficient and orderly material transport. The integrated ordered membrane electrode can effectively maintain the morphology of the ordered array, reduce the destruction of the ordered structure caused by hot pressing, and has a small contact interface impedance, so it has great potential for improvement in all aspects. Nanoimprint is one of the common methods for constructing nanostructures on the surface of Nafion films. The method is simple and controllable, and can effectively improve the three-phase boundary, so it has been widely used in the preparation of nanostructured PEMs.[132,133] Bae *et al.* prepared a nanostructured Nafion film with a linear patterned surface by thermal imprint lithography (TIL).[134] SEM images showed that the pre-designed template pattern was printed in high fidelity on the surface of the Nafion film. Due to the increase in the PEM/CL interface area, the catalyst can better expose the active site, thereby improving the catalytic performance and significantly enhancing the performance of PEMFCs. In order to improve the triple-phase interface of the cathode CL, Zhou's group integrated a Nafion array membrane with a large specific surface area and high proton conductivity

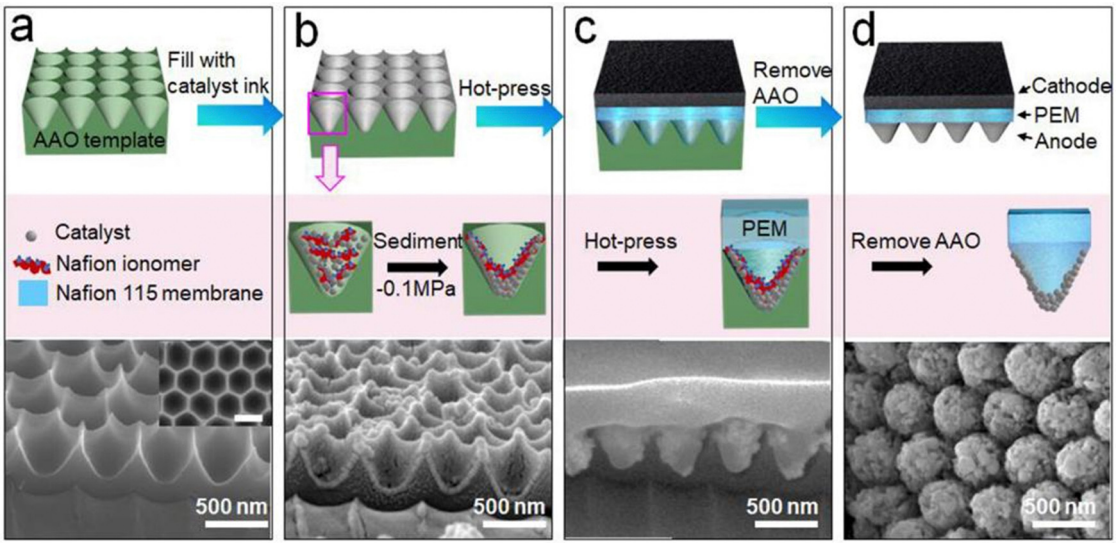

Fig. 13 Preparation procedure of the MEA with GTAs. (a) SEM image of a cross section of the AAO template. The inset shows the top view of the template. (b) Cross-sectional SEM image of the dried template filled with catalyst and ionomer. (c) SEM image of the composite structure of the CL, PEM, and the template. (d) SEM image of the tapered arrays after removing the template. Reproduced with permission from ref. 138. Copyright 2022 American Chemical Society.

into the cathode CL, thereby creating an ordered MEA. They then filled the Nafion array with Pt NPs by an impregnation process.[135] However, the sputtering method often leads to the agglomeration of Pt NPs, which will reduce the proton migration efficiency.[136] In order to prevent this phenomenon, the authors utilized the principle that sulfonic acid groups readily adsorb to the surface of Pt. They covered the Pt NPs with Nafion, enhancing proton conduction and thereby speeding up the proton transfer efficiency.[137] With a Pt loading of 61.4 μg cm^{-2}, the peak power density of the prepared PEMFC reached an impressive 843 mW cm^{-2}, much higher than that of the PEMFC without Nafion (710 mW cm^{-2}) in the cathode CLs. In addition, this PEMFC can operate continuously and stably for 100 h without significant voltage attenuation. In summary, a proton transfer channel is established at the triple-phase interface by adsorbing Nafion on the surface of the Pt catalyst in the cathode CL, offering an effective strategy for the development of PEMFCs.

PEM surface ordering is a promising technique for water electrolysis, which can effectively solve the problems of insufficient catalyst utilization, limited mass transfer and high ohmic resistance caused by the degradation of MEAs. Dong *et al.* proposed the preparation of a novel ordered MEA based on an anode 3D membrane/CL interface and gradient tapered array (GTA) (Fig. 13).[138] Nano-imprinting technology and a simple static strategy were used to cast the catalyst ink slowly on the porous AAO template surface. Then, the cathode catalyst coated film and the anode CL template are hot-pressed to make MEAs. Through the overall design, it has a maximum three-phase interface, fast mass transfer and GTA CL. Compared with conventional MEA with Ir loading of 2 mg cm^{-2}, the ECSA with this unique ordered structure is greatly increased, and the overpotential of mass transfer and ohmic polarization is reduced by 13.9% and 8.7%, respectively. Moreover, the MEA with GTA can work stably for more than 300 h at a current density of 1 A cm^{-2}, which has excellent stability, and provides a new strategy for the ordered MEA design of high-performance PEMWE. Similarly, Zhou's group employed AAO templates and magnetron sputtering to fabricate an ordered MEA featuring a conical Nafion array. This design incorporates a Nafion gradient distribution, strong CL/PEM interfaces, and vertically aligned channels, leading to enhanced performance.[139] For this ordered MEA, the Nafion membrane with a cone array structure on the surface significantly improves the catalyst utilization efficiency and reduces the Ir loading to 20.0 μg cm^{-2}, greatly reducing Ir catalyst usage and cost. Magnetron sputtering evenly deposits the catalyst onto the Nafion array membrane, preserving the ordered structure while providing a large number of high-speed, vertically aligned channels for proton transport. This design optimizes catalyst utilization and enhances proton conductivity, contributing to improved overall performance. This ordered MEA exhibits 8.7 times higher ECSA compared to a conventional MEA with 1.0 mg cm^{-2} Ir loading. It achieves a remarkable mass activity of 168 000 mA mg_{Ir}^{-1} cm^{-2} at 2.0 V, surpassing the performance of most reported PEMWEs. This MEA demonstrates excellent durability at a current density of 500 mA cm^{-2}. However, existing ordered polymer structures are typically single-component systems. The proton conductivity of Nafion (0.15 S cm^{-1}) is nearly 100 times lower than that of the Ir catalyst,[140,141] which affects the PEMWE performance of the corresponding MEAs.[142,143] While the ordered proton conductor structure facilitates efficient proton transport and improves PEMWE performance, the smooth surface of the Nafion cone array limits contact between the catalysts and PEMs. This limitation restricts further performance improvements in PEMWE.[138] Therefore, Zhou's group developed a novel MEA incorporating TiO_2 NPs within a conical Nafion array, resulting in a

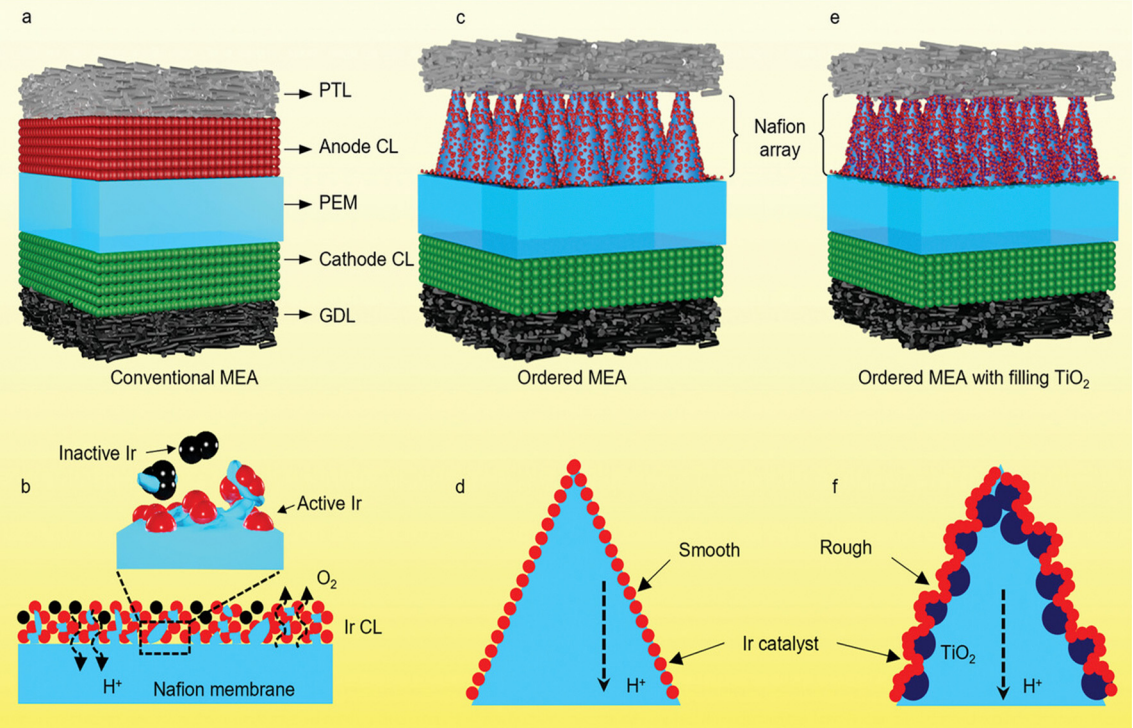

Fig. 14 (a) Conventional MEA. (b) Cross-section images of conventional MEA. (c) Ordered MEA. (d) Cross-section images of ordered MEA. (e) Ordered MEA with TiO_2 doping. (f) Cross-section images of ordered MEA with TiO_2 doping. Reproduced with permission from ref. 144. Copyright 2023 Wiley.

roughened surface (Fig. 14).[144] This mixed ordered MEA exhibits a significantly enhanced surface roughness of 3.39 nm, 2.64 times higher than the ordered MEA without TiO_2 NPs. This increased roughness significantly improves the interface contact between the CLs and Nafion membranes. At 2.0 V, the MEA has a current density of 2.48 A cm^{-2} with a catalyst loading of 14.4 μg_{Ir} cm^{-2}. This work paves the way for further research aimed at optimizing the interface between CLs and membranes, leading to improved performance in PEMWE.

4. Conclusions and outlook

In this feature article, we describe in detail the development of ordered MEAs in the field of hydrogen energy, mainly concerning the classification of ordered MEAs and its application in fuel cells and water electrolysis for hydrogen production. Initial advancements in ordered MEAs focused on 1D ordered nanomaterials such as nanowires, nanotubes and nanofibers. These nanomaterials, with their high specific surface area and fast material transport capacity, effectively address the issue of limited electrocatalyst utilization in traditional MEAs, boosting their WE performance. However, creating an entirely ordered structure for multi-mass delivery remains a challenge, hindering their use in demanding applications. As a solution, various 3D ordered MEAs have been reported in the applications of fuel cells and water electrolysis. These can be broadly classified into ordered supports, ordered catalysts and ordered membranes. The new generation of ordered MEA designs can significantly improve the performance of MEAs in all aspects, reduce the load of precious metal catalyst, enhance the transport at the triple-phase boundary of CLs and greatly lower the production cost. The CL's excellent surface wettability facilitates product gas release and electrolyte penetration. Although significant progress has been made in the development of nanostructured MEAs, challenges remain:

(1) Immature preparation technology: ordered MEA technology is still in its developmental stage, with limitations in preparation processes, material selection, and control, hindering its scalability for commercial applications. In addition, the need for precise control during preparation creates a risk of microscopic defects and structural instability, hindering large-scale production and adoption of ordered MEAs.

(2) Durability and stability: during long-term operation, degradation can occur within the MEA, affecting its stability and performance. Electrocatalysts, catalyst supports, and ion exchange membranes are susceptible to corrosion and dissolution, reducing the active area. Fluctuations in temperature and pressure can cause electrode material expansion, contraction, or deformation, potentially leading to catalyst detachment. Furthermore, particle deposition and electrolyte residue can block the GDL, impeding gas diffusion and electrode performance.

(3) Practical application: current strategies for ordered MEAs are primarily laboratory-based and face challenges in scaling up for industrial production. Under operational conditions, vibration and shock can induce structural loosening or breakage within the MEA. Moreover, high production costs hinder the attainment of desired performances in large-scale manufacturing.

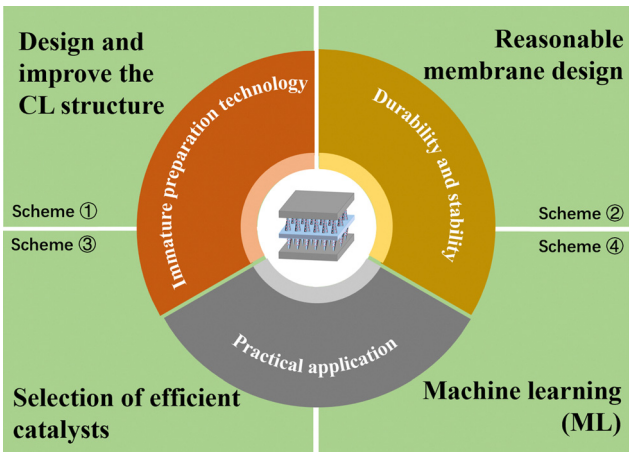

Fig. 15 Schematic of the challenges and possible improvements for ordered MEAs.

Furthermore, in order to develop high-quality ordered MEA, we can explore the following aspects (Fig. 15): (i) design and improve the CL structure: the thickness of CL will affect the mass transfer effect. A thinner CL, while ensuring adequate mechanical strength, can enhance mass transfer by reducing diffusion distances. This leads to faster ion migration and an increased electrochemical reaction rate. (ii) Reasonable membrane design: while thicker membranes enhance durability, they also hinder ion transport due to longer diffusion paths, leading to larger ohmic impedance and reduced current density. Finding the optimal membrane thickness is crucial for achieving high performance in ordered MEAs. To address the limitations of traditional homogeneous PEMs or AEMs, enhanced composite ion exchange membranes, such as expanded polytetrafluoroethylene (ePTFE) reinforced membranes, offer a solution by combining high ion conductivity with improved durability. (iii) Selection of efficient catalysts: traditional precious metal electrocatalysts, while highly active, suffer from high costs and significant dissolution issues during long-term operation. This has driven intense research into non-precious metal electrocatalysts, leading to the development of materials with both excellent durability and high catalytic activity.[145,146] These promising alternatives not only enhance the catalytic activity of reactions such as the ORR and HER but also enable long-term operation at high current densities, significantly improving the stability and durability of ordered MEAs. (iv) Machine learning (ML): ML may significantly accelerate the development of ordered MEAs. ML trains big models using known data, *e.g.*, nanostructures, supports, catalysts and membranes, to build relationships between complex ordered structures and MEA performance, which can facilitate the combination of artificial intelligence technologies for researchers.

Author contributions

N. Hua wrote the original draft, C. Zhang, W. Zhang, and X. Yao collected textual and diagram information and Prof. H. Qian (supervisor) reviewed and edited the manuscript.

Data availability

No primary research results, software or code have been included and no new data were generated or analysed as part of this review.

Conflicts of interest

There are no conflicts to declare.

Acknowledgements

This work was supported by the National Natural Science Foundation of China (22279157).

Notes and references

1 P. Zhou, I. A. Navid, Y. Ma, Y. Xiao, P. Wang, Z. Ye, B. Zhou, K. Sun and Z. Mi, *Nature*, 2023, **613**, 66–70.
2 M. Yu, K. Wang and H. Vredenburg, *Int. J. Hydrogen Energy*, 2021, **46**, 21261–21273.
3 M. Dumortier and S. Haussener, *Energy Environ. Sci.*, 2015, **8**, 3069–3082.
4 M. K. Lee, S. Choi, H. Park, T. H. Lee, S. A. Lee, J. W. Yang, S. G. Ji, W. S. Cheon, S. H. Ahn, S. Y. Kim, M. Shokouhimehr, J. Y. Kim and H. W. Jang, *Energy Technol.*, 2023, **11**, 2201203.
5 D. Bertasini, F. Battista, F. Rizzioli, N. Frison and D. Bolzonella, *Renewable Energy*, 2023, **206**, 386–396.
6 S. Krevor, H. de Coninck, S. E. Gasda, N. S. Ghaleigh, V. de Gooyert, H. Hajibeygi, R. Juanes, J. Neufeld, J. J. Roberts and F. Swennenhuis, *Nat. Rev. Earth Environ.*, 2023, **4**, 102–118.
7 S. E. Jun, Y.-H. Kim, J. Kim, W. S. Cheon, S. Choi, J. Yang, H. Park, H. Lee, S. H. Park, K. C. Kwon, J. Moon, S.-H. Kim and H. W. Jang, *Nat. Commun.*, 2023, **14**, 609.
8 Y. Shang, S. Chen, N. Chen, Y. Li, J. Lai, Y. Ma, J. Chen, F. Wu and R. Chen, *Energy Environ. Sci.*, 2022, **15**, 2653–2663.
9 M. D. Allendorf, V. Stavila, J. L. Snider, M. E. Witman, K. Brooks, B. L. Tran and T. Autrey, *Nat. Chem.*, 2022, **14**, 1214–1223.
10 S. E. Jun, J. K. Lee, S. Ryu and H. W. Jang, *ChemCatChem*, 2023, **15**, e202300926.
11 L. Fan, Z. Tu and S. H. Chan, *Energy Rep.*, 2021, **7**, 8421–8446.
12 S. E. Jun, S. Choi, J. Kim, K. C. Kwon, S. H. Park and H. W. Jang, *Chin. J. Catal.*, 2023, **50**, 195–214.
13 S. E. Jun, J. K. Lee and H. W. Jang, *Energy Adv.*, 2023, **2**, 34–53.
14 N. A. Burton, R. V. Padilla, A. Rose and H. Habibullah, *Renewable Sustainable Energy Rev.*, 2021, **135**, 110255.
15 F. Yang, M. J. Kim, M. Brown and B. J. Wiley, *Adv. Energy Mater.*, 2020, **10**, 2001174.
16 J. Kim, S. Choi, J. Cho, S. Y. Kim and H. W. Jang, *ACS Mater. Au*, 2022, **2**, 1–20.
17 M. Noussan, P. P. Raimondi, R. Scita and M. Hafner, *Sustainability*, 2021, **13**, 298.
18 L. Wan, Z. Xu, Q. Xu, H. Xu and B. Wang, *Energy Environ. Sci.*, 2023, **16**, 1384–1430.
19 K. Zeng and D. Zhang, *Prog. Energy Combust. Sci.*, 2010, **36**, 307–326.
20 A. Buttler and H. Spliethoff, *Renewable Sustainable Energy Rev.*, 2018, **82**, 2440–2454.
21 V. A. Panchenko, Yu. V. Daus, A. A. Kovalev, I. V. Yudaev and Yu. V. Litti, *Int. J. Hydrogen Energy*, 2023, **48**, 4551–4571.
22 J. C. Ehlers, A. A. Feidenhans'l, K. T. Therkildsen and G. O. Larrazábal, *ACS Energy Lett.*, 2023, **8**, 1502–1509.
23 M. Chatenet, B. G. Pollet and D. R. Dekel, *et al.*, *Chem. Soc. Rev.*, 2022, **51**, 4583–4762.
24 J. Wang, Y. Gao, H. Kong, J. Kim, S. Choi, F. Ciucci, Y. Hao, S. Yang, Z. Shao and J. Lim, *Chem. Soc. Rev.*, 2020, **49**, 9154–9196.
25 M. Mandal, *ChemElectroChem*, 2020, **8**, 36–45.
26 Y. Luo, Z. Zhang, M. Chhowalla and B. Liu, *Adv. Mater.*, 2022, **34**, 2108133.

27 Q. Wang, C.-Q. Xu, W. Liu, S.-F. Hung, H. Bin Yang, J. Gao, W. Cai, H. M. Chen, J. Li and B. Liu, *Nat. Commun.*, 2020, **11**, 4246.
28 J. K. Lee, J. H. Seo, J. Lim, S. W. Park and H. W. Jang, *ACS Mater. Lett.*, 2024, **6**, 2757–2786.
29 S. Stiber, H. Balzer, A. Wierhake, F. J. Wirkert, J. Roth, U. Rost, M. Brodmann, J. K. Lee, A. Bazylak, W. Waiblinger, A. S. Gago and K. A. Friedrich, *Adv. Energy Mater.*, 2021, **11**, 2100630.
30 S. Slade, S. A. Campbell, T. R. Ralph and F. C. Walsh, *J. Electrochem. Soc.*, 2002, **149**, A1556–A1564.
31 L. Wan, M. Pang, J. Le, Z. Xu, H. Zhou, Q. Xu and B. Wang, *Nat. Commun.*, 2022, **13**, 7956.
32 S. A. Lee, S. E. Jun, S. H. Park, K. C. Kwon, J. H. Kang, M. S. Kwon and H. W. Jang, *EES Catal.*, 2024, **2**, 49–70.
33 F. Barbir, *Fuel Cell Technol.*, Springer, London, 2002–2018, pp. 27–51.
34 H. Tang, S. Wang, M. Pan, S. P. Jiang and Y. Ruan, *Electrochim. Acta*, 2007, **52**, 3714–3718.
35 L. Wan, Z. Xu, Q. Xu, P. Wang and B. Wang, *Energy Environ. Sci.*, 2022, **15**, 1882.
36 E. H. Majlan, D. Rohendi, W. R. W. Daud, T. Husaini and M. A. Haque, *Renewable Sustainable Energy Rev.*, 2018, **89**, 117–134.
37 A. Bonnefont, P. Ruvinskiy, M. Rouhet, A. Orfanidi, S. Neophytides and E. Savinova, *Wiley Interdiscip. Rev.: Energy Environ.*, 2014, **3**, 505–521.
38 M. K. Debe, S. M. Hendricks, G. D. Vernstrom, M. Meyers, M. Brostrom, M. Stephens, Q. Chan, J. Willey, M. Hamden, C. K. Mittelsteadt, C. B. Capuano, K. E. Ayers and E. B. Anderson, *J. Electrochem. Soc.*, 2012, **159**, K165–K176.
39 A. Bonakdarpour, K. Stevens, G. D. Vernstrom, R. Atanasoski, A. K. Schmoeckel, M. K. Debe and J. R. Dahn, *Electrochim. Acta*, 2007, **53**, 688–694.
40 M. K. Debe, R. T. Atanasoski and A. J. Steinbach, *ECS Trans.*, 2011, **41**, 937–954.
41 D. F. van der Vliet, C. Wang, D. Tripkovic, D. Strmcnik, X. F. Zhang, M. K. Debe, R. T. Atanasoski, N. M. Markovic and V. R. Stamenkovic, *Nat. Mater.*, 2012, **11**, 1051–1058.
42 G. Wang, L. Zou, Q. Huang, Z. Zhou and H. Yang, *J. Mater. Chem. A*, 2019, 7(16), 9447–9477.
43 C. Koenigsmann, A. C. Santulli, K. Gong, M. B. Vukmirovic, W.-P. Zhou, E. Sutter, S. S. Wong and R. R. Adzic, *J. Am. Chem. Soc.*, 2011, **133**, 9783–9795.
44 M. Li, Z. Zhao, T. Cheng, A. Fortunelli, C.-Y. Chen, R. Yu, Q. Zhang, L. Gu, B. V. Merinov, Z. Lin, E. Zhu, T. Yu, Q. Jia, J. Guo, L. Zhang, W. A. Goddard III, Y. Huang and X. Duan, *Science*, 2016, **354**, 1414–1419.
45 L. Bu, S. Guo, X. Zhang, X. Shen, D. Su, G. Lu, X. Zhu, J. Yao, J. Guo and X. Huang, *Nat. Commun.*, 2016, **7**, 11850–11859.
46 Y. S. Kim, H. J. Kim and W. B. Kim, *Electrochem. Commun.*, 2009, **11**, 1026–1029.
47 M.-T. Sung, M.-H. Chang and M.-H. Ho, *J. Power Sources*, 2014, **249**, 320–326.
48 R. Wang, D. C. Higgins, M. A. Hoque, D. Lee and Z. Chen, *Sci. Rep.*, 2013, **3**, 2431.
49 S. Sun, F. Jaouen and J.-P. Dodelet, *Adv. Mater.*, 2008, **20**, 3900–3904.
50 H. J. Kim, Y. S. Kim, M. H. Seo, S. M. Choi, J. Cho, G. W. Huber and W. B. Kim, *Electrochem. Commun.*, 2010, **12**, 32–35.
51 Y. S. Kim, H. J. Kim and W. B. Kim, *Electrochem. Commun.*, 2009, **11**, 1026–1029.
52 H. Liang, X. Cao, F. Zhou, C. Cui, W. Zhang and S. Yu, *Adv. Mater.*, 2011, **23**, 1467.
53 C. Liang, P. Zou, A. Nairan, Y. Zhang, J. Liu, K. Liu, S. Hu, F. Kang, H. J. Fan and C. Yang, *Energy Environ. Sci.*, 2020, **13**, 86–95.
54 H. Zhu, Z. Zhu, J. Hao, S. Sun, S. Lu, C. Wang, P. Ma, W. Dong and M. Du, *Adv. Mater.*, 2022, **34**, e2105350.
55 H. Kim, H. Park, D.-K. Kim, S. Oh, I. Choi and S.-K. Kim, *ACS Sustainable Chem. Eng.*, 2019, **7**, 8265–8273.
56 Z. Tang, H. Y. Ng, J. Lin, A. T. S. Wee and D. H. C. Chua, *J. Electrochem. Soc.*, 2010, **157**, B245–B250.
57 W. Zhang, J. Chen, G. F. Swiegers, Z.-F. Ma and G. G. Wallace, *Nanoscale*, 2010, **2**, 282–286.
58 S. M. Andersen, M. Borghei, P. Lund, Y.-R. Elina, A. Pasanen, E. Kauppinen, V. Ruiz, P. Kauranen and E. M. Skou, *Solid State Ionics*, 2013, **231**, 94–101.
59 S. Gahlot and V. Kulshrestha, *ACS Appl. Mater. Interfaces*, 2015, **7**, 264–272.
60 A. Bharti and G. Cheruvally, *J. Power Sources*, 2017, **360**, 196–205.
61 A. K. Roy and C.-T. Hsieh, *Electrochim. Acta*, 2013, **87**, 63–72.
62 B. Fang, M.-S. Kim, J. H. Kim, M. Y. Song, Y.-J. Wang, H. Wang, D. P. Wilkinson and J.-S. Yu, *J. Mater. Chem.*, 2011, **21**, 8066–8073.
63 X. Hu, R. Wang, P. Sun, Z. Xiang and X. Wang, *ACS Sustainable Chem. Eng.*, 2019, **7**, 19426–19433.
64 P. K. R. Holzapfel, M. Bühler, D. Escalera-López, M. Bierling, F. D. Speck, K. J. J. Mayrhofer, S. Cherevko, C. V. Pham and S. Thiele, *Small*, 2020, **16**, 2003161.
65 F. L. Yuan, H. K. Yu and H. J. Ryu, *Electrochim. Acta*, 2004, **50**, 685–691.
66 Z. R. Ismagilov, M. A. Kerzhentsev, N. V. Shikina, A. S. Lisitsyn, L. B. Okhlopkova, C. N. Barnakov, M. Sakashita, T. Iijima and K. Tadokoro, *Catal. Today*, 2005, **102**, 58–66.
67 L. Calvillo, M. Gangeri, S. Perathoner, G. Centi, R. Moliner and M. J. Lazaro, *J. Power Sources*, 2009, **192**, 144–150.
68 Y. Wang, J. Jin, S. Yang, G. Li and J. Qiao, *Electrochim. Acta*, 2015, **177**, 181–189.
69 J. Choi, K. M. Lee, R. Wycisk, P. N. Pintauro and P. T. Mather, *ECS Trans.*, 2008, **16**, 1433.
70 J. Choi, K. M. Lee, R. Wycisk, P. N. Pintauro and P. T. Mather, *Macromolecules*, 2008, **41**, 4569.
71 L. Chen, H. L. Tao, J. R. Li and M. Pan, *Int. J. Energy Res.*, 2013, **37**, 879.
72 C. Busacca, S. C. Zignani, A. Di Blasi, O. Di Blasi, M. Lo Faro, V. Antonucci and A. S. Aricó, *Int. J. Hydrogen Energy*, 2019, **44**, 20987–20996.
73 S. Kang, K. Ham and J. Lee, *Electrochim. Acta*, 2020, **353**, 136521.
74 A. Caillard, C. Charles, R. Boswell and P. Brault, *J. Phys. D: Appl. Phys.*, 2008, **41**, 185307.
75 W. Li, X. Wang, Z. Chen, M. Waje and Y. Yan, *Langmuir*, 2005, **21**, 9386.
76 T. Hatanka, H. Nakanishi, S. Matsumoto and Y. Morimoto, *ECS Trans.*, 2006, **3**, 277.
77 W. Zhang, J. Chen, A. I. Minett, G. F. Swiegers, C. O. Too and G. G. Wallace, *Chem. Commun.*, 2010, **46**, 4824–4826.
78 L. Xuan, D. Mei and C. Zhou, *Ind. Chem. Mater.*, 2024, **1**, 1400035.
79 Z. X. Lu, Y. Shi, C.-F. Yan, C.-Q. Guo and Z.-D. Wang, *Int. J. Hydrogen Energy*, 2017, **42**, 3572–3578.
80 Z. Ren, L. Jin, L. Deng, R. Ming, A. Zhang, X. Zhou, B. Chai and Y. Zhu, *Sustainable Energy Fuels*, 2019, **3**, 2321–2328.
81 Z. X. Lu, Y. Shi, P. Gupta, X. P. Min, H. Y. Tan, Z. D. Wang, C. Q. Guo, Z. Q. Zou, H. Yang, S. Mukerjee and C. F. Yan, *Electrochim. Acta*, 2020, **348**, 136302.
82 G. Jiang, H. Yu, Y. Li, D. Yao, J. Chi, S. Sun and Z. Shao, *ACS Appl. Mater. Interfaces*, 2021, **13**, 15073–15082.
83 J. Qin, Y. Lv, G. Han, H. Liu, Y. Li, H. Zhang, X. Zhou, K. Xing, T. Li, C. Sun, C. Wang, Q. Zhou, R. Wu, D. Wang and Y. Song, *Chem. Eng. J.*, 2024, **479**, 147913.
84 Y. Zeng, X. Guo, Z. Shao, H. Yu, W. Song, Z. Wang, H. Zhang and B. Yi, *J. Power Sources*, 2017, **342**, 947–955.
85 H. Sun, Z. Yan, F. Liu, W. Xu, F. Cheng and J. Chen, *Adv. Mater.*, 2020, **32**, 1806326.
86 J. Chi, H. Yu, B. Qin, L. Fu, J. Jia, B. Yi and Z. Shao, *ACS Appl. Mater. Interfaces*, 2017, **9**, 464–471.
87 G. Ding, H. Lee, Z. Li, J. Du, L. Wang, D. Chen and L. Sun, *Adv. Energy Sustainability Res.*, 2023, **4**, 2200130.
88 J. T. Davis, B. S. Jayathilake and S. Chandrasekaran, *Sci. Rep.*, 2024, **14**, 22662.
89 J. C. Bui, J. T. Davis and D. V. Esposito, *Sustainable Energy Fuels*, 2020, **4**, 213–225.
90 M. K. Debe, S. M. Hendricks, G. D. Vernstrom, M. Meyers, M. Brostrom, M. Stephens, Q. Chan, J. Willey, M. Hamden, C. K. Mittelsteadt, C. B. Capuano, K. E. Ayers and E. B. Anderson, *J. Electrochem. Soc.*, 2012, **159**, K165–K176.
91 M. K. Debe, R. T. Atanasoski and A. J. Steinbach, *ECS Trans.*, 2011, **41**, 937–954.
92 R. J. Ziegler, J. H. Thomas, M. K. Debe, G. M. Haugen, A. J. Steinbach, K. Debe, M. Haugen, J. Steinbach, H. Thomas and J. Ziegler, US5879827-A, 1999.
93 M. K. Debe, R. J. Ziegler, S. M. Hendricks, M. Debe, R. Ziegler and S. Henfricks, US2008020923-A1, 2008.
94 M. Zhang, J. J. Li, M. Pan and D. S. Xu, *Acta Phys.-Chim. Sin.*, 2011, **7**, 1685.

95 Y. Zeng, Z. Shao, H. Zhang, Z. Wang, S. Hong, H. Yu and B. Yi, *Nano Energy*, 2017, **34**, 344–355.
96 R. Phillips and C. W. Dunnill, *RSC Adv.*, 2016, **6**, 100643.
97 I. Fouzaï, *J. Mater. Chem. A*, 2021, **9**, 11096–11123.
98 Y. Zeng, *J. Mater. Chem. A*, 2018, **6**, 6521–6533.
99 J. Liu, D. Zhu, Y. Zheng, A. Vasileff and S.-Z. Qiao, *ACS Catal.*, 2018, **8**, 6707–6732.
100 M. Tang, S. Zhang and S. Chen, *Chem. Soc. Rev.*, 2022, **51**, 1529–1546.
101 X. Deng, C. Huang, X. Pei, B. Hu and W. Zhou, *Int. J. Hydrogen Energy*, 2022, **47**, 1529–1542.
102 L. Wan, M. Pang, J. Le, Z. Xu, H. Zhou, Q. Xu and B. Wang, *Nat. Commun.*, 2022, **13**, 7956.
103 L. Wan, Z. Xu, Q. Xu, P. Wang and B. Wang, *Energy Environ. Sci.*, 2022, **15**, 1882–1892.
104 L. Wan, J. Liu, D. Lin, Z. Xu, Y. Zhen, M. Pang, Q. Xu and B. Wang, *Energy Environ. Sci.*, 2024, **17**, 3396–3408.
105 Y. Sone, P. Ekdunge and D. Simonsson, *J. Electrochem. Soc.*, 1996, **143**, 1254–1259.
106 M. N. Silberstein, P. V. Pillai and M. C. Boyce, *Polymer*, 2011, **52**, 529–539.
107 W. Li, J. Jiang, H. An, S. Dong, Z. Yue, H. Qian and H. Yang, *ACS Appl. Energy Mater.*, 2021, **4**, 2732–2740.
108 B. Xue, M. Zhu, S. Fu, P. Huang, H. Qian and P. Liu, *J. Membr. Sci.*, 2023, **673**, 121263.
109 W. Li, R. Zhang, X. Zhao, Z. Yue, H. Qian and H. Yang, *J. Mater. Chem. A*, 2023, **11**, 4547–4558.
110 G. Chao, Z. Zhang, Z. Lv, E. Yang, R. Gao, Q. Ju, H. Gao, C. Niu, H. Qian, K. Geng and N. Li, *J. Membr. Sci.*, 2024, **700**, 122674.
111 B. Xue, Z. Zheng, H. Qian, Z. Wang and J. Yan, *Macromolecules*, 2024, **57**, 3376–3386.
112 K. Wang, S. McDermid, J. Li, N. Kremliakova, P. Kozak, C. Song, Y. Tang, J. Zhang and J. Zhang, *J. Power Sources*, 2008, **184**, 99–103.
113 J. Lu, H. Tang, C. Xu and S. P. Jiang, *J. Mater. Chem.*, 2012, **22**, 5810–5819.
114 Y. Lin, H. Li, C. Liu, W. Xing and X. Ji, *J. Power Sources*, 2008, **185**, 904–908.
115 T. Yuan, L. Pu, Q. Huang, H. Zhang, X. Li and H. Yang, *Electrochim. Acta*, 2014, **117**, 393–397.
116 J. Zheng, Q. He, C. Liu, T. Yuan, S. Zhang and H. Yang, *J. Membr. Sci.*, 2015, **476**, 571–579.
117 B. Dong, L. Gwee, D. Salas-De La Cruz, K. I. Winey and Y. A. Elabd, *Nano Lett.*, 2010, **10**, 3785.
118 H. Tang, Z. Wan, M. Pan and S. P. Jiang, *Electrochem. Commun.*, 2007, **9**, 2003–2008.
119 Z. Chai, C. Wang, H. Zhang, C. M. Doherty, B. P. Ladewig, A. J. Hill and H. Wang, *Adv. Funct. Mater.*, 2010, **20**, 4394–4399.
120 K. Wang, S. McDermid, J. Li, N. Kremliakova, P. Kozak, C. Song, Y. Tang, J. Zhang and J. Zhang, *J. Power Sources*, 2008, **184**, 99–103.
121 J. Lu, H. Tang, C. Xu and S. P. Jiang, *J. Mater. Chem.*, 2012, **22**, 5810–5819.
122 J. Lu, S. Lu and S. P. Jiang, *Chem. Commun.*, 2011, **47**, 3216–3218.
123 M. S. Cha, J. E. Park, S. Kim, S.-H. Shin, S. H. Yang, S. J. Lee, T.-H. Kim, D. M. Yu, S. So, K. M. Oh, Y. E. Sung, Y.-H. Cho and J. Y. Lee, *J. Mater. Chem. A*, 2022, **10**, 9693–9706.
124 A. N. Lai, Y. Z. Zhuo, C. X. Lin, Q. G. Zhang, A. M. Zhu, M. L. Ye and Q. L. Liu, *J. Membr. Sci.*, 2016, **502**, 94–105.
125 Q. Ge, X. Liang, L. Ding, J. Hou, J. Miao, B. Wu, Z. Yang and T. Xu, *J. Membr. Sci.*, 2019, **573**, 595–601.
126 L. Zhu, X. Peng, S. L. Shang, M. T. Kwasny, T. J. Zimudzi, X. Yu, N. Saikia, J. Pan, Z. K. Liu, G. N. Tew, W. E. Mustain, M. Yandrasits and M. A. Hickner, *Adv. Funct. Mater.*, 2019, **29**, 1902059.
127 Y. Zhu, L. Ding, X. Liang, M. A. Shehzad, L. Wang, X. Ge, Y. He, L. Wu, J. R. Varcoe and T. Xu, *Energy Environ. Sci.*, 2018, **11**, 3472–3479.
128 W. Chen, T. Li, X. Yan, X. Wu, Y. Zhang, X. Wang, F. Zhang, S. Zhang and G. He, *J. Membr. Sci.*, 2021, **629**, 119293.
129 W. Chen, X. Wang, T. Li, X. Yan, X. Wu, Y. Zhang, F. Zhang, S. Zhang and G. He, *J. Membr. Sci.*, 2021, **640**, 119815.
130 L. Liu, L. Bai, Z. Liu, S. Miao, J. Pan, L. Shen, Y. Shi and N. Li, *J. Membr. Sci.*, 2023, **665**, 121135.
131 C. Hu, X. Deng, X. Dong, Y. Hong, Q. Zhang and Q. Liu, *J. Membr. Sci.*, 2021, **619**, 118806.
132 Y. Zhang, J. Lu, H. Zhou, T. Itoh and R. Maeda, *J. Microelectromech. Syst.*, 2008, **17**, 1020–1028.
133 M. Aizawa, H. Gyoten, A. Salah and X. Liu, *J. Electrochem. Soc.*, 2010, **157**, B1844–B1851.
134 J. W. Bae, Y.-H. Cho, Y.-E. Sung, K. Shin and J. Y. Jho, *J. Ind. Eng. Chem.*, 2012, **18**, 876–879.
135 S. Pan, Q. Wen, X. Dan, Y. Li, F. Ning, C. He, W. Li, M. Shen, L. He, B. Tian, Y. Zhang, W. Feng, Y. Zou, X. Zhou and A. C. S. Appl, *Energy Mater.*, 2023, **6**, 763–772.
136 S. Kabir, T. Van Cleve, S. Khandavalli, S. Medina, S. Pylypenko, S. Mauger, M. Ulsh, K. C. Neyerlin and A. C. S. Appl, *Energy Mater.*, 2021, **4**, 3341–3351.
137 K. Kodama, K. Motobayashi, A. Shinohara, N. Hasegawa, K. Kudo, R. Jinnouchi, M. Osawa and Y. Morimoto, *ACS Catal.*, 2018, **8**, 694–700.
138 S. Dong, C. Zhang, Z. Yue, F. Zhang, H. Zhao, Q. Cheng, G. Wang, J. Xu, C. Chen, Z. Zou, Z. Dou and H. Yang, *Nano Lett.*, 2022, **22**, 9434–9440.
139 B. Tian, Y. Li, Y. Liu, F. Ning, X. Dan, Q. Wen, L. He, C. He, M. Shen and X. Zhou, *Nano Lett.*, 2023, **23**, 6474–6481.
140 E. Pollak, I. Genish, G. Salitra, A. Soffer, L. Klein and D. Aurbach, *J. Phys. Chem. B*, 2006, **110**, 7443.
141 D. Böhm, M. Beetz, C. Gebauer, M. Bernt, J. Schröter, M. Kornherr, F. Zoller, T. Bein and D. Fattakhova-Rohlfing, *Appl. Mater. Today*, 2021, **24**, 101134.
142 G. Jiang, H. Yu, Y. Li, D. Yao, J. Chi, S. Sun and Z. Shao, *ACS Appl. Mater. Interfaces*, 2021, **13**, 15073.
143 P. Wang, T. Jia and B. Wang, *J. Power Sources*, 2020, **474**, 228621.
144 Y. Liu, B. Tian, F. Ning, Y. Li, C. Zhao, C. He, Q. Wen, X. Dan, Z. Chai, W. Li, M. Shen, L. He, W. Li and X. Zhou, *Adv. Energy Mater.*, 2024, **14**, 2303353.
145 C. Song, Y. Liu, Y. Wang, S. Tang, W. Li, Q. Li, J. Zeng, L. Chen, H. Peng and Y. Lei, *Sci. China Mater.*, 2021, **64**, 1662–1670.
146 Y. He, Z. Kang, J. Li, Y. Li and X. Tian, *Ind. Chem. Mater.*, 2023, **1**, 312–331.

